frontiers | Frontiers in Earth Science

TYPE Original Research
PUBLISHED 27 September 2022
DOI 10.3389/feart.2022.997145

OPEN ACCESS

EDITED BY
Fei Huang,
Hunan University of Science and Technology, China

REVIEWED BY
Liang Cheng,
China Merchants Chongqing Communications Technology Research & Design Institute Co., Ltd., China
Qingsheng Bai,
Freiberg University of Mining and Technology, Germany

*CORRESPONDENCE
Chengwei Liu,
liuchengwei12@126.com

SPECIALTY SECTION
This article was submitted to Environmental Informatics and Remote Sensing, a section of the journal Frontiers in Earth Science

RECEIVED 18 July 2022
ACCEPTED 05 September 2022
PUBLISHED 27 September 2022

CITATION
Yang J, Zheng X, Liu C, Zhai W, Liu H and Zhang P (2022), Study on improving the gas extraction efficiency by deep-hole pre-split blasting in Wulunshan Coal Mine, Guizhou.
Front. Earth Sci. 10:997145.
doi: 10.3389/feart.2022.997145

Study on improving the gas extraction efficiency by deep-hole pre-split blasting in Wulunshan Coal Mine, Guizhou

Junwei Yang[1,2], Xigui Zheng[1,2], Chengwei Liu[2]*, Wenjie Zhai[3], Hongyang Liu[2,4] and Peng Zhang[2]

[1]School of Mines, China University of Mining and Technology, Xuzhou, Jiangsu, China, [2]School of Mining and Mechanical Engineering, Liupanshui Normal University, Liupanshui, Guizhou, China, [3]Shanxi Heshuntianchi Energy Co. Ltd, Jinzhong, Shanxi, China, [4]College of Energy and Mining Engineering, Shandong University of Science and Technology, Qingdao, Shandong, China

Due to the low permeability of the coal seam and the low gas extraction rate in conventional boreholes in the Wulunshan Coal Mine in Guizhou, in this study, the deep-hole pre-split blasting method is applied to study the improvement of the gas extraction efficiency by increasing the permeability of the coal seam. The study comprehensively expounds the process in which the deep-hole pre-split blasting method is applied to improve the gas extraction efficiency and proposes a numerical simulation method that combines ANSYS/LS-DYNA and COMSOL Multiphysics. Using the method, the initiation of blasting fracture channels and the subsequent influence on the gas extraction range have been comprehensively and directly researched and analyzed. Finally, some theoretical research has been verified by field experiments. According to the recorded simulation of the Wulunshan Coal Mine, the exposed area of the blasting borehole was 42 times the size of the conventional drilling borehole, and the pressure relief space was 1,050 times that of the conventional drilling borehole, which can connect about 32 m^3 of coal. Compared with conventional drilling boreholes, in the process of gas extraction, the control range of the controlled pressure reduction was 4–7 times, the range of gas pressure reaching the standard was 25 times, and the peak pressure was reduced by 3–5 times. The average gas concentration was 1.85 times that of conventional boreholes, and the cumulative gas extraction volume of blasting boreholes was 4.48 times that of conventional boreholes. The research results prove that the application of blasting and permeability enhancement in the coal seam with a high gas content and low permeability can effectively improve the gas extraction efficiency in the Wulunshan Coal Mine in Guizhou.

KEYWORDS

blasting, coal seam permeability enhancement, gas drainage, LS-DYNA, COMSOL, engineering practice

1 Introduction

Gas is not only one of the main factors that induce coal mine disasters and the greenhouse effect but is also a valuable clean energy source (Li et al., 2019; Fan et al., 2021; Liang et al., 2021; Lu et al., 2022). Therefore, the development and utilization of gas resources can not only improve the safe, efficient, and clean production of mines but also optimize China's energy structure and relieve environmental issues (Li et al., 2020). China is very rich in gas resources, the amount of which with buried depth within 2,000 m is 10.87×10^{14} m^3, equivalent to the proven reserves of conventional natural gas resources on land in China, accounting for about 13% of the total gas resources in the world (Sun et al., 2018). Also, the gas resources in Guizhou province rank second in the country. However, because the coal resource-enriched area in Guizhou province is located in the composite part of the Neo-Cathaysian third fold belt and the southern part of the subsidence belt and the Nanling zonal structural belt, there are more developed folds and faults, complex coal seam structure, high ground stress, poor permeability, and other characteristics (Bai and Tu, 2019; Zhao et al., 2022). As a result, the conventional gas extraction rate is low, and it is difficult to achieve the expected effect.

The fundamental measure to improve the gas extraction rate is to create a large-scale fracture network in the coal seam to provide pressure relief space for the coal seam and gas drainage and migration channels, subsequently increasing the permeability of the coal seam (Bai et al., 2017; Qi et al., 2021). In recent years, relevant experts and scholars at home and abroad have carried out a large number of theoretical analyses, laboratory experiments, numerical simulations, similar simulations, and engineering experiments to improve coal seam permeability. A variety of coal seam fracturing and permeability-inducing technologies such as deep-hole blasting (Kurlenya et al., 2020; Liu et al., 2022a), water jet slotting (Huang et al., 2020; Huang et al., 2021), hydraulic fracturing (Bai et al., 2020; Wang et al., 2022a), CO_2 phase transition fracturing (Shang et al., 2022), tree-type borehole (Zuo et al., 2022), protective layer mining (Wang et al., 2022b), and ultrasonic waves to improve permeability (Li et al., 2021) have been used. Fair effects brought by these attempts have been achieved. Among them, deep-hole blasting is widely used because of its simple process and obvious permeability-increasing effect. However, during the blasting, the blasting point is located in the deep part of the borehole, and rock blasting is instantaneously dynamic. As a result, the existing research mostly reflects the implementation effect of this technical method on the final gas extraction rate. In contrast, the process where blasting and permeability increasing are incurred is difficult to visualize.

Therefore, in order to deeply study the whole process of deep-hole pre-split blasting to improve the coal seam permeability and increase the gas extraction rate, this study comprehensively expounds the process of deep-hole pre-split blasting for coal seams to improve the gas extraction rate and proposes the use of ANSYS/LS-DYNA. The numerical simulation method combined with LS-DYNA and COMSOL Multiphysics can comprehensively and intuitively study and analyze the fabrication of the blast fracture channel and its influence on the gas drainage range. Finally, the theoretical research is verified by field experiments. This study will provide a theoretical basis for optimizing the deep-hole blasting method in coal seams and improving the cracking mechanism of deep-hole blasting, which has important reference significance for improving the coal seam permeability, preventing mine gas disasters, and developing and utilizing gas resources.

2 The theory of permeability enhancement in deep-hole pre-split blasting

The permeability enhancement in deep-hole pre-split blasting uses the explosive load generated by the explosive to act on the coal, causing the coal to crack and loosen, resulting in the formation of a crushing ring, a crack ring, and a vibration ring in the radial direction from the inside to the outside of the coal around the blasting hole (Huang and Li, 2015); meanwhile, the blasting stress wave acts on the coal to adsorb gas, providing energy for gas desorption (Yang et al., 2018).

2.1 Explosion shock wave cavitation and initial fracturing

After the explosive is detonated in the rock mass, the detonation wave propagates on a spherical surface from the center of the explosive at the same speed. After the explosive is detonated, the pressure of the explosive gas is as high as 10^9~10^{10}Pa. The compressive strength of hard rock is only about 10^8Pa, which is far less than the explosion gas pressure. Therefore, under the influence of high-temperature and high-pressure explosive gas, the rock adjacent to the charge is strongly compressed, the structure is completely destroyed, the particles are crushed, and even liquefied. The entire rock undergoes radial movement due to the extrusion of the explosive gas, forming an explosion cavity, and a shock wave propagating with ultrasonic waves begins to form in this area. The peak pressure of the shock wave front is expressed as follows:

$$P_m = 53.3\left(\frac{W^{1/3}}{r}\right)^{1.13}\left(\frac{Q_i}{Q_T}\right)^{1.13/3}. \quad (1)$$

In the formula, Qi——explosive heat, kc/kg;Q_T——TNT heat, 1,000 kc/kg;W——load amount, kg;r——distance from the center of the explosive, m.

When the peak pressure of the shock wave front is greater than the strength limit of the coal-rock mass, the coal-rock mass forms an initial fracture under the action of the shock wave (Huang and Hu, 2018). With the increase in the distance between the shock wave front and the charge, the shock wave pressure decreases rapidly. When it is at a certain distance from the charge, the overpressure is lower than the strength limit of the rock, and the strong deformation and crushing phenomenon gradually disappear, the main structure of the rock remains unchanged, and the initial crack stops expanding.

2.2 Quasi-static pressure promotes crack propagation

After the initial cracking, with the forward propagation and attenuation, the shock wave is no longer the main driving force for the crack expansion. At this time, the shock wave generated by the explosion propagates rapidly in the blasthole, forms on the wall of the blasthole, and travels to the blasthole. The reflected wave propagating inside and the subsequent blasting gas work together to continuously expand and compress the original media in the blasthole. In this process, the explosive gas continues to expand, the volume increases, and the pressure decreases; the initial air is compressed, the volume decreases, and the pressure rises (Ding et al., 2020). At the time when the pressure of the explosion gas reduced by the expansion is equal to the pressure of the original air in the blast hole, an equilibrium state is reached at this time, the expansion and compression process ends, and a quasi-static pressure is formed in the blast hole. The quasi-static pressure wedges into the opened initial crack, producing stress concentration at the crack tip and further expanding the crack. According to the theory of fracture mechanics, the stress intensity factor at the crack tip is expressed as follows (Koguchi et al., 2015):

$$K_I = PF(\xi)\sqrt{\pi(r+a)}, \tag{2}$$

where P ——the quasi-static pressure in the blasthole;r——the inner radius of the blast hole;a——cracking length;$F(\xi)$—the correction factor associated with r, and $\xi = \frac{r+a}{r}$

As the crack expands, the quasi-static pressure P in the blasthole gradually decreases, and when the stress intensity factor near the crack tip is less than or equal to the dynamic fracture tenacity of the rock, the crack stops expanding.

2.3 The criterion for crack stop

$$K_I = PF(\xi)\sqrt{\pi(r+a)} \le K_{Id}, \tag{3}$$

where K_{Id} is the dynamic fracture tenacity of the initial rock, then

$$P \le \frac{K_{Id}}{F(\xi)\sqrt{\pi(r+a)}}. \tag{4}$$

At this point, the cracking is stopped, and the blasting crack propagation ends.

2.4 Stress wave propagation enhances gas desorption

As the blast shock wave penetrates the coal, a stress wave is formed to propagate in the coal, and the peak pressure of the wavefront is as follows:

$$P_b = P_m \frac{\rho_c C_m + \rho_0 D_0}{2\rho_c C_m}, \tag{5}$$

where P_m——the peak pressure of the wavefront, Pa; $\rho_c C_m$——coal wave impedance; ρ_c and C_m are coal density and longitudinal wave velocity, respectively; $\rho_0 D_0$——wave impedance; when the shock wave velocity is D_0, ρ_0 and D_0 are air density and longitudinal wave velocity, respectively.

The stress wave propagating in the coal is a longitudinal wave, and the propagation direction of the wave is consistent with the vibration direction of the coal mass point, which causes the coal of different densities to longitudinally vibrate, resulting in the diameter changes of the coal capillary tubes in the porous medium. The change is conducive to the desorption and diffusion of coal seam gas; the coal-rock skeleton and the fluid in it also vibrate. Due to the different densities of the skeleton and the fluid, the resulting acceleration and amplitude are different, causing the fluid–solid interface to move relatively. When the movement is strong enough, a tendency to fracture and crack is formed, which weakens the adhesion between gas and coal and is conducive to the desorption of gas from coal. At the same time, when the stress wave propagates in the coal and causes the coal to vibrate, a certain amount of energy is absorbed by the internal friction between the particles due to the viscosity of the coal. The temperature of the coal increases, the thermal motion of methane gas molecules intensifies, and the collision of free gas molecules also increases, which improves the desorption efficiency of coal adsorption gas (Cheng et al., 2021).

To sum up, the deep-hole pre-split blasting method, *via* load blasting, creates a pressure relief space in the coal, constructs the gas migration crack channel, strengthens gas desorption, and forms the positive cycle of "coal mass pressure relief, fracture evolution → permeability enhancement in coal mass, strengthening gas desorption, gushing→drainage to reduce gas pressure→coal pressure relief, and fracture evolution". Gas permeability in the coal mass is, thus, reduced, and the gas extraction rate is, thus, increased.

TABLE 1 Coal material parameters.

G	S_{max}	A	B	C	N	D_1	D_2	K_1	K_2
34.91 GPa	7.0	0.79	1.6	0.007	0.61	0.046	1.0	85 GPa	−171 GPa
ρ	P_{crush}	μ_{crush}	P_{lock}	μ_{lock}	EF_{min}	f_C'	F_s	T	K_3
2840Kg/m3	50 MPa	0.016	800 MPa	0.1	0.01	150 MPa	−1	7.59 MPa	208 GPa

3 Numerical simulation research on the extraction range of deep-hole pre-split blasting

Explosion is the dynamic process of instantaneous high-speed, high-temperature, high-pressure, and high-energy release. The current technical means and testing instruments are not sufficient to reflect on-site rock blasting and explosion crack evolution in gas extraction and gas flow and pressure range through experimental methods. In order to deeply analyze deep-hole pre-split blasting, the evolution of blasting cracks in drilling holes, and the process of drilling extraction, and to further verify the theoretical analysis, the nonlinear dynamic analysis program ANSYS/LS-DYNA was used to simulate the evolution process of drilling fracturing and its final patterns. Then, the simulated fracture patterns were imported into physical modeling by COMSOL Multiphysics software, and the extraction range of conventional drilling and blasting drilling was comparatively analyzed and studied by COMSOL Multiphysics software.

3.1 Numerical simulation of the borehole blasting fracture

The #8 coal seam of the Wulunshan Coal Mine was selected as the research object. By building a model according to the physical and mechanical parameters and occurrence conditions of the #8 coal seam, the fracture patterns of the #8 coal seam were recorded after deep-hole pre-split blasting, which was to be used in the later comparison and simulation of gas extraction between conventional holes and blast holes.

3.1.1 Numerical computation model

3.1.1.1 Geometric model

The model is simulated by volume elements. Since the shape of the blast hole is cylindrical and radially symmetric, it is identical on each section of the blast hole axis. Therefore, in order to reduce the calculation time, the model was only established with the necessary thickness instead of the full size so as to obtain the evolution of cracks on the cross section with two-dimensional simulation results. The size of the model was 10000×10000×10 mm, and the blasthole was arranged at the center of the model. The diameter of the blasthole was 73 mm. The bottom and left sides of the model were constrained by displacement. A horizontal stress of 14.5 MPa was applied to the right side, and a vertical stress of 23.3 MPa was applied to the upper side. The explosives were of coupled charges.

3.1.1.2 Coal model

The Johnson–Holmquist model was used as the coal material, and the parameters of the model are shown in Table 1.

*MAT_ADD_EROSION keyword was added to the k-file as a failure criterion to define the compressive strength and principal stress failure of the coal (Huang et al., 2018). When the coal compressive strength reaches the set value or the principal stress reaches the set value, it fails, thus simulating the failure of coal blasting.

3.1.1.3 Explosive material parameters

*MAT_HIGH_EXPLOSIVE_BURN was used as the model of explosive materials, and the JWL equation of state was used to calculate the detonation pressure:

$$P = A\left(1 - \frac{\omega}{R_1 V}\right)e^{-R_1 V} + B\left(1 - \frac{\omega}{R_2 V}\right)e^{-R_2 V} + \frac{\omega E}{V}, \quad (6)$$

where P—detonation pressure; E—internal energy of the explosion product; V—relative volume of the detonation product; A, B, R_1, R_2, and ω—property constants of selected explosives.

The selected explosive materials and state equation parameters are shown in Table 2.

3.1.2 Computational results and analyses

The overall process of the simulation results is shown in Figure 1.

After blasting, the shock wave formed by the explosion propagated from the center of the blast hole to the coal. First, a blasting cavity centered on the original blasting hole was formed. With the propagation of the shock wave, the blasting cavity space no longer developed, and main blasting fractures were formed, following the development of the shock wave in up, down, left, and right directions. Since the coal seam was under the vertical maximum principal stress, the main fractures in the vertical direction developed more rapidly than in the horizontal direction. At about 300 ms, the main fractures are almost fully developed. Secondary cracks in coal were then formed under ground stress and by subsequent explosion loads. The secondary

10.3389/feart.2022.997145

TABLE 2 Explosive materials and state equation parameters.

Density/g·cm-3	Detonation speed/cm·us-1	Detonation pressure/GPa	A/GPa	B/GPa	R1	R2	ω	E/GPa
1.60	1.993	55.5	540.9	9.373	4.5	1.1	0.35	8

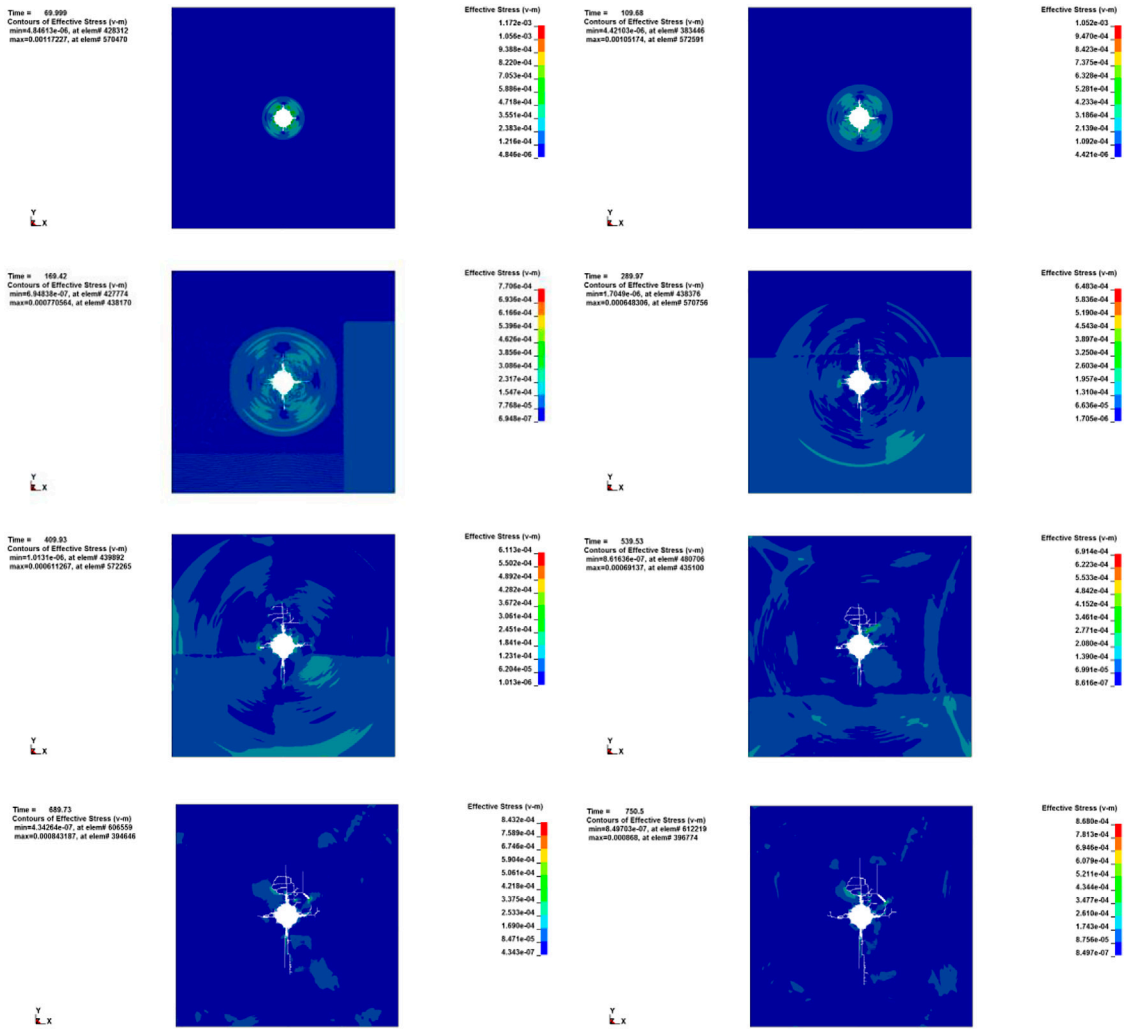

FIGURE 1
Original image of simulation results.

cracks were likewise more developed in the vertical direction and less in the horizontal direction due to ground stress. The entire process of the blast fracture lasted about 760 ms. Finally, an explosion cavity with a diameter of 1 m was formed, and an ellipse-shaped fracture ring with a vertical length of 6 m and a horizontal width of 3.2 m was formed, as shown in Figure 2.

Compared with the boreholes before blasting, in the conventional borehole with a diameter of 73 mm at a length of 1 m, the exposed area of the coal was about 0.3 m^2, the pressure relief space was 0.004 m^3, and there was no crack channel extending to the deeper part of the coal; after blasting, the exposed area of the coal formed by the blast cavity with a diameter of 1 m was 12.6 m^2, 42 times that of conventional boreholes, the cavity volume was 4.2 m^3, and the pressure relief space was 1,050 times that of conventional boreholes, and a volume of about 32 m^3 of coal was connected.

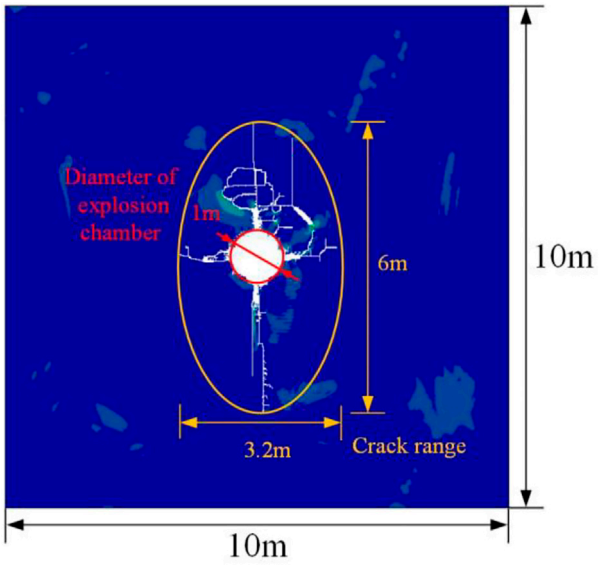

FIGURE 2
Analysis of simulation results.

Therefore, compared with conventional borehole drilling, blasting borehole drilling can provide a larger exposed area in the coal, more pressure relief space, and connect a larger range of coal, which are more conducive to the increase of coal permeability and efficient gas extraction.

3.2 Numerical simulation of the extraction range of blasting boreholes

After completing the numerical simulation of blasting fracturing, the crack coordinate script file of the simulation results obtained in 3.1 was imported into AutoCAD to generate the calculation model graphics. The further generated AutoCAD model was imported into COMSOL Multiphysics to form a model of blasting borehole drilling. Comparison simulation experiments of the gas extraction efficiency with boreholes and conventional boreholes were performed.

3.2.1 Numerical computation model

3.2.1.1 Model size and meshing

Since the extraction range is wider than the fracture range, in order to facilitate the study of the extraction range of the two types of boreholes, in extraction simulation, the established geometric model was expanded to 16000×16000 mm. A free triangular mesh is adopted in the calculation model. After the model governing equations, boundary conditions, initial values, and meshes are all set, the solution can be solved after setting the solution parameters in the solver parameter setting. The transient solver was used in the calculation; the solution time in the time step was set to 0: 86,400: 86400000, the relative tolerance was 0.01, and the absolute tolerance was 0.001; the maximum BDF order is 5. The schematic diagram of the geometric model and boundary conditions is shown in Figure 3.

Since the model is perfectly symmetric in space and the gas weight is small, the influence of the angle of inclination on gas extraction was ignored (Liu et al., 2022b). Therefore, a plane model was built.

3.2.1.2 Calculation parameters

The elastic modulus E is calculated by the following formula:

$$E = 0.4029R_0 + 3.4724, \quad (7)$$

where: R_0 —coal seam vitrinite reflectance, dimensionless;

During the calculation, the parameters of the coal seam were selected with reference to the #8 coal seam of the Wulunshan Coal Mine, as shown in Table 3 as follows.

3.2.2 Calculation results and analyses

This study mainly focuses on the comparative study of the gas extraction range of conventional borehole drilling and blasting borehole drilling and studies the reduction of gas pressure in different drilling holes under the change of extraction duration. After 30, 60, and 90 days of extraction, the gas pressure drop ranges under the two borehole types were investigated. The simulation results are shown in Figure 4.

In the subsequent analyses, relevant data from the X and Y directions that are perpendicular to each other were studied. The gas pressures in the simulation results and the distances from the center borehole were exported, and the data in these two directions were used to draw the gas cloud map. A combined analysis was performed.

As shown in Figure 5, the median pressure of 1.76 MPa of the original gas (2.78 MPa) and extraction standard (0.74 MPa) were defined as the criteria for the control range of pressure reduction the trend of the gas pressure reduction curve of conventional boreholes did not change much with the extraction time, and they were all similar to logarithmic curves. The pressure dropped slowly outside the range of 1 m from the drilling hole, while within 1m, the pressure dropped rapidly.

The gas pressure reduction curve trend of blasting holes was also relatively stable with the extraction time. It is a hyperbolic curve that first decreases slowly, then rapidly decreases in the range of about 4 m, and gradually becomes gentler after the lowest value. It was observed that the pressure drop range of blasting holes was larger. After 30 days, it reached a radius of 4 m; after 60 days, it reached 5 m, and after 90 days, the pressure drop range was close to 7 m, close to

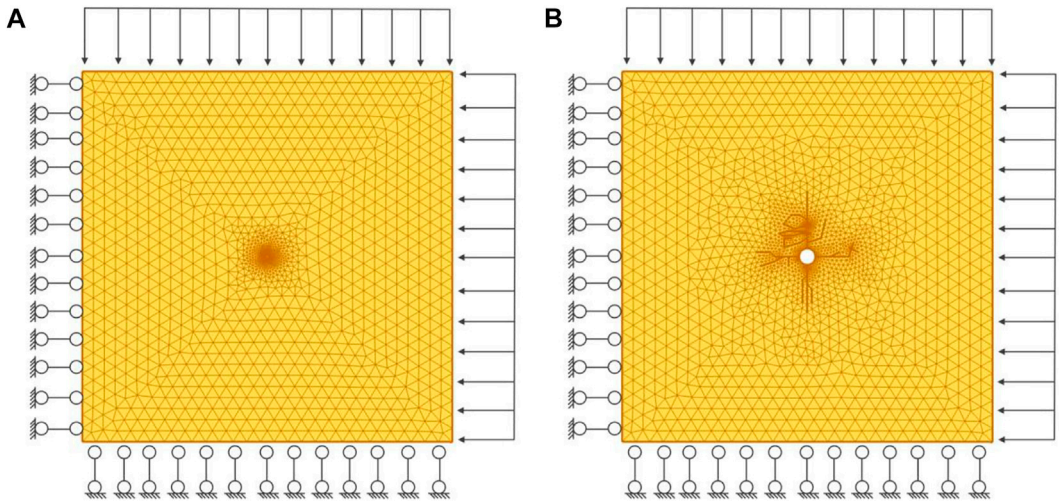

FIGURE 3
Section diagrams of the model and meshing.

TABLE 3 Calculation parameters of the model.

Parameter	Value
Coal elastic modulus E	$4.06 \times 10^9 Pa$
Coal Poisson's ratio v	0.28
Coefficient of thermal expansion of coal β	$0.000116\ m^3/m^3 \cdot K$
Gas dynamic viscosity μ	$1.08 \times 10^{-5} Pa \cdot s$
Coal density	$1400 kg/m^3$
Initial porosity of coal ϕ_0	0.062
Initial permeability of coal k_0	$2.5 \times 10^{-17} m^2$
Initial gas pressure p_0	$2.8 MPa$
Adsorption constant a	$28.47 m^3/t$
Adsorption constant b	$0.0077 kPa^{-1}$
Specific heat capacity of coal C_{pc}	$4186 J/(kg \cdot K)$
Coal heat transfer coefficient k_c	$5 W/(m \cdot K)$
Gas heat transfer coefficient k_g	$0.731 W/(m \cdot K)$
Specific heat capacity of gas C_{pg}	$2227 J/(kg \cdot K)$

the simulated edge range, and the pressure drop range also increased significantly with the increase of extraction time. The pressure reduction control range of blasting drilling is relatively large, and with the increase in extraction time, it reaches 4 to 7 times that of conventional boreholes.

According to the "Regulations on the Prevention and Control of Coal and Gas Outbursts", this study adopts a gas pressure lower than 0.74 MPa as the inspection index for the scope of the extraction standard. After 30 days, the up-to-standard rate of gas pressure was low in conventional boreholes, only about 0.18 m in both X and Y directions, roughly a circular range; after 60 and 90 days of extraction, the pressure drop ranges were not obvious, also only 0.2 m in diameter. In comparison, after 30, 60, and 90 days of extraction, the up-to-standard rates of gas pressure were similar in blasting boreholes; all dropped rapidly below the inspection index after entering the blasting fractures. The range was about 4.4 m in the X direction and 5 m in the Y direction. Blasting boreholes can significantly increase the range of gas pressure compliant to the standard, which is about 25 times that of conventional boreholes.

The original gas pressure at the selected location for the simulation was 2.8 MPa, and the simulated boundary is 8 m away from the extraction hole. The peak pressures after extraction from the two types of drilling holes were compared.

The pressure in conventional boreholes was 2.74 MPa after 30 days, 2.63 MPa after 60 days, and 2.52 MPa after 90 days, which reduced by 2.14%, 6.07%, and 10%, respectively. However, in blasting boreholes, the pressures were 2.47 MPa after 30 days, 2.13 MPa after 60 days, and 1.87 MPa after 90 days, which decreased by 11.79%, 23.92%, and 33.21%, respectively. In comparison, blasting boreholes had a significant reduction effect on the peak pressure within the simulation range, and the reduction range was 3–5 times that of conventional drilling.

4 Field extraction experiment of deep-hole presplit blasting

4.1 Overview of the test site

The Wulunshan Coal Mine is located in Nayong County, Guizhou province. The first coal seam to be mined is the No.

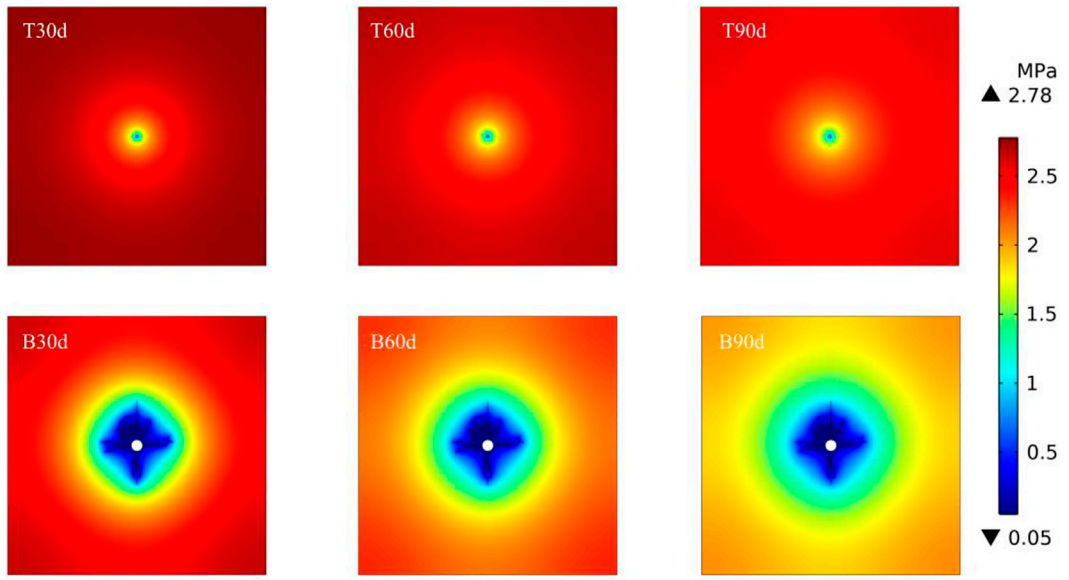

FIGURE 4
Original image of simulation results.

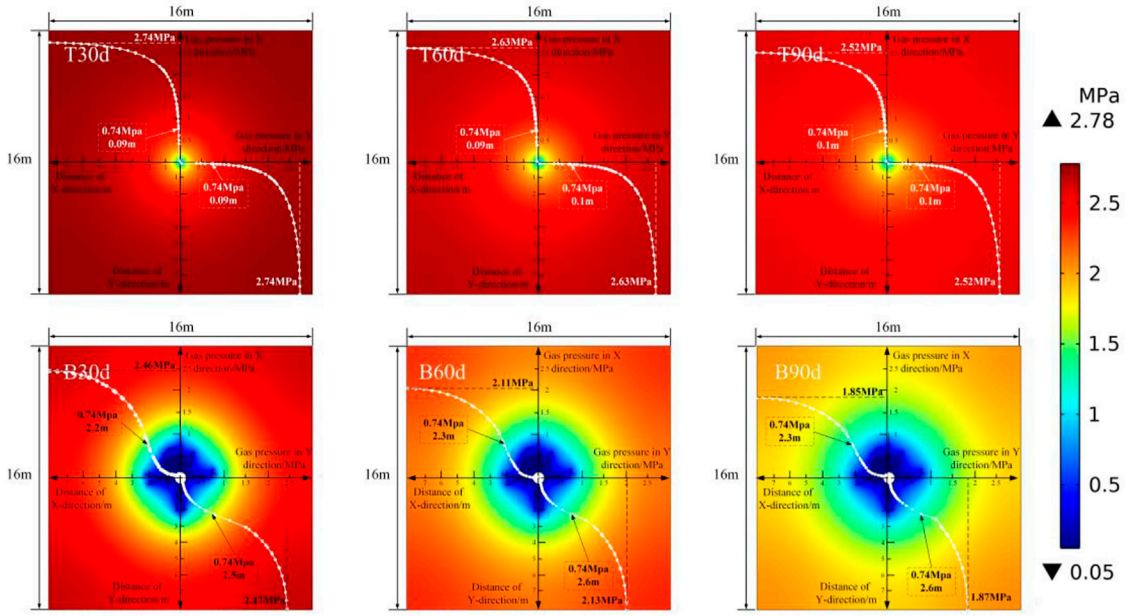

FIGURE 5
Simulation result analysis diagram.

8 coal seam, which has a low permeability coefficient and a large attenuation coefficient of borehole gas emission. It is a mine that is difficult to extract. The basic parameters of No. 8 coal seam gas are shown in Table 4.

The test site is located at 1807 Transport Lane, where experimental boreholes are drilled along the mining seam. A set of blasting holes and conventional holes were selected for comparative testing.

TABLE 4 Basic parameters of coal seam gas in the first mining seam No. 8.

Coal seam number	8
Original gas content (m^3/t)	14.47
Initial velocity of gas release Δp	16.44
Gas pressure MPa	3.0
Coal seam failure type	III
Coal firmness factor f	0.78
Coal seam permeability coefficient (m^2/(MPa^2·d))	0.00002–0.1061
Attenuation coefficient of borehole gas emission (d^{-1})	0.1757–1.0531

4.2 Test results and analyses

The sealing quality of the sealed drilling holes was tested by pressure injection, and the gas extraction parameters of blasting boreholes and conventional boreholes were regularly tested by optical gas detectors. The trend of the gas concentration was drawn using the measured data on boreholes in the extraction area.

In November 2020, the gas concentration of blasting boreholes and conventional boreholes was tested every 2 days. The results are shown in Table 4, and the cumulative gas extraction volume is shown in Table 5.

It can be seen from Table 5, 6 and Figure 6, 7 that the average concentration of the gas extracted from conventional boreholes was only 37.81%, and the monthly average concentration of the gas extracted from blasting boreholes was 69.82%, 1.85 times that of conventional boreholes. The cumulative gas extraction volume of conventional boreholes was 206 m^3, and the cumulative gas extraction volume of blasting boreholes was 922 m^3, 4.48 times that of conventional boreholes. Through data analysis, compared with traditional drilling, the gas extraction efficiency after blasting is significantly improved, and the gas extraction concentration and cumulative gas extraction volume are significantly improved, which indicates that blasting can effectively improve the gas extraction efficiency in high gas content and low-permeability coal seams.

TABLE 5 Gas extraction concentration of blasting boreholes and conventional boreholes.

Date of measuring	Blasting borehole (%)	Conventional borehole (%)	Date of measuring	Blasting borehole (%)	Conventional borehole (%)
11.01	82.80	52.40	11.17	68.60	40.20
11.03	80.50	50.60	11.19	65.20	36.80
11.05	80.60	49.60	11.21	65.10	33.60
11.07	75.60	49.30	11.23	63.20	30.90
11.09	76.20	48.30	11.25	62.80	27.60
11.11	73.80	41.90	11.27	62.10	27.30
11.13	72.90	40.30	11.29	59.50	20.50
11.15	70.40	40.50	11.31	57.80	15.20

TABLE 6 Cumulative gas extraction volume of blasting boreholes and conventional boreholes.

Date of measuring	Blasting borehole (m)	Conventional borehole (m)	Date of measuring	Blasting borehole (m)	Conventional borehole (m)
11.01	2^3	2^3	11.17	565^3	178^3
11.03	58^3	13^3	11.19	627^3	185^3
11.05	136^3	65^3	11.21	670^3	190^3
11.07	218^3	121^3	11.23	735^3	193^3
11.09	287^3	133^3	11.25	767^3	195^3
11.11	373^3	165^3	11.27	812^3	201^3
11.13	456^3	167^3	11.29	864^3	204^3
11.15	532^3	172^3	11.31	922^3	206^3

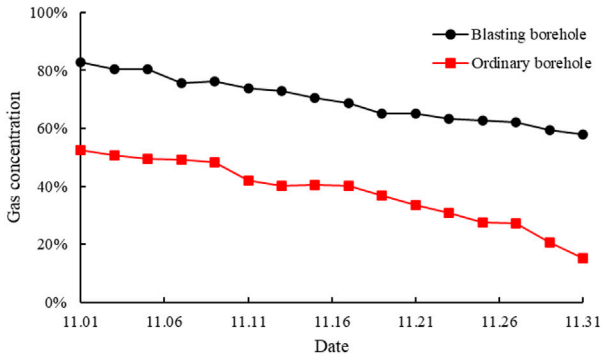

FIGURE 6
| Comparison of the gas extraction concentration between blasting boreholes and conventional boreholes.

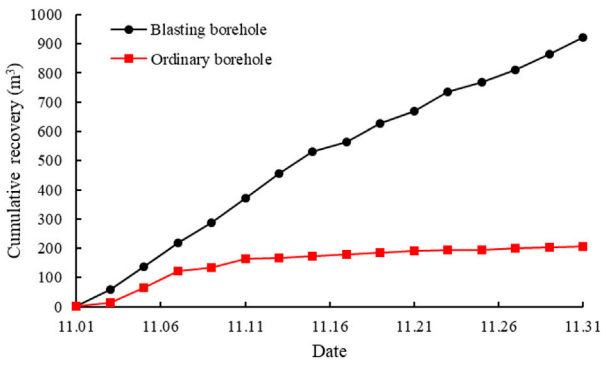

FIGURE 7
Comparison of the cumulative gas extraction volume between blasting boreholes and conventional boreholes.

5 Conclusion

1) The deep-hole pre-split blasting method uses the blasting load to create pressure relief space for coal mass, build gas migration fracture channels, and strengthen gas desorption, forming a positive circulation of "coal mass pressure relief, fracture evolution → permeability-enhancing of coal mass, enhanced gas desorption, gushing →gas pressure reduced in extraction → coal pressure relief, and fracture evolution". Thus, reduced coal permeability and higher extraction of gas are achieved.
2) LS-DYNA was used to simulate the evolution process and final patterns of fractures in conventional boreholes and blasting boreholes. The simulation results showed that, compared with conventional boreholes without blasting, the exposed area of coal was 42 times that of conventional boreholes, and the pressure relief space is the same as that of conventional drilling. It is 1,050 times the size of the borehole. At the same time, the fracture propagation connected about 32 m^3 of coal. Therefore, compared with conventional boreholes, blasting boreholes can provide a larger exposed area of coal, more pressure relief space, and connect a larger range of coal, which is more conducive to the increase of coal permeability and efficient gas extraction.
3) By importing the crack coordinate script file of the simulation results obtained in LS-DYNA into AutoCAD, the calculation model graphics were generated, and the generated AutoCAD model was further imported into COMSOL Multiphysics to form a drilling model of the blasting fracture borehole. The comparison simulation experiment was carried out to study the gas extraction efficiency of blasting boreholes and conventional boreholes. The experimental results showed that the pressure reduction control range of blasting boreholes is relatively large, and with the increase of extraction time, it reached 4–7 times that of conventional boreholes; blasting boreholes can significantly increase the range of gas pressure, reaching the standard, 25 times that of conventional boreholes; the peak pressure reduction effect of blasting boreholes is obvious in the simulation range, 3–5 times that of conventional boreholes.
4) The feasibility of the deep-hole pre-split blasting method was verified using theoretical analysis and numerical simulation experiments. The test results showed that the average gas concentration in blasting boreholes was 1.85 times that of conventional boreholes, and the cumulative gas extraction volume in blasting boreholes was 4.48 times that of conventional boreholes. Field experiments showed that the application of blasting and permeability enhancement can effectively improve the gas extraction efficiency in coal seams with a high gas content and low permeability.

Data availability statement

The raw data supporting the conclusion of this article will be made available by the authors, without undue reservation.

Author contributions

JY, XZ, CL, HL, and PZ designed and implemented numerical simulation experiments and wrote the manuscript. WZ, JY, and CL were responsible for field testing and data recording.

Funding

The work is jointly supported by the Science and Technology Department of Guizhou Province Fund (Qiankehe Basis [2019]

1291), the Education Department of Guizhou Province Fund (Qianjiaohe KY Zi [2019] 073, Qianjiao XKTJ [2020] 23), and the Academician Workstation of Liupanshui Normal University (Qiankehe Platform Talent-YSZ[2021]001).

Conflict of Interest

WZ is employed by Shanxi Heshuntianchi Energy Co. Ltd., China.

The remaining authors declare that the research was conducted in the absence of any commercial or financial relationships that could be construed as a potential conflict of interest.

Publisher's note

References

Bai, Q., Liu, Z., Zhang, C., and Wang, F. (2020). Geometry nature of hydraulic fracture propagation from oriented perforations and implications for directional hydraulic fracturing. *Comput. Geotechnics* 125 (10), 103682. doi:10.1016/j.compgeo.2020.103682

Bai, Q., and Tu, S. (2019). A general review on longwall mining-induced fractures in near-face regions. *Geofluids* 2019 (19), 1–22. doi:10.1155/2019/3089292

Bai, Q., Tu, S., Wang, F., and Zhang, C. (2017). Field and numerical investigations of gateroad system failure induced by hard roofs in a longwall top coal caving face. *Int. J. Coal Geol.* 173, 176–199. doi:10.1016/j.coal.2017.02.015

Cheng, Y., Liu, Q., and Ren, T. (2021). Gas adsorption–desorption properties of coal. *Coal Mech.* 16, 111–150. doi:10.1007/978-981-16-3895-4_4

Ding, C., Yang, R., Lei, Z., Chen, C., and Zheng, C. (2020). Experimental study on blasting energy distribution and utilization efficiency using water jet test. *Energies* 13, 5340. doi:10.3390/en13205340

Fan, C., Yang, L., Wang, G., Huang, Q., Fu, X., and Wen, H. (2021). Investigation on coal skeleton deformation in CO2 injection enhanced CH4 drainage from underground coal seam. *Front. Earth Sci.* 9, 766011. doi:10.3389/feart.2021.766011

Huang, B., and Li, P. (2015). Experimental investigation on the basic law of the fracture spatial morphology for water pressure blasting in a drillhole under true triaxial stress. *Rock Mech. Rock Eng.* 48 (4), 1699–1709. doi:10.1007/s00603-014-0649-y

Huang, Fei, and Hu, Bin (2018). Macro/microbehavior of shale rock under the dynamic impingement of a high-pressure supercritical carbon dioxide jet. *RSC Adv.* 8, 38065–38074. doi:10.1039/C8RA07480A

Huang, Fei, Li, Shuqing, Zhao, Yanlin, and Liu, Yong (2018). A numerical study on the transient impulsive pressure of a water jet impacting nonplanar solid surfaces. *J. Mech. Sci. Technol.* 32 (9), 4209–4221. doi:10.1007/s12206-018-0819-z

Huang, Fei, Mi, Jianyu, Li, Dan, and Wang, Rongrong (2020). Impinging performance of high-pressure water jets emitting from different nozzle orifice shapes. *Geofluids* 8, 1–14. doi:10.1155/2020/8831544

Huang, F., Mi, J., Li, D., Wang, R., and Zhao, Z. (2021). Comparative investigation of the damage of coal subjected to pure water jets, ice abrasive water jets and conventional abrasive water jets. *Powder Technol.* 394, 909–925. doi:10.1016/j.powtec.2021.08.079

Koguchi, H., Yokoyama, K., and Luangarpa, C. (2015). Variation of stress intensity factor along a small interface crack front in singular stress fields. *Int. J. Solids Struct.* 71, 156–168. doi:10.1016/j.ijsolstr.2015.06.016

Kurlenya, M. V., Tsupov, M. N., Savchenko, A. V., and Pugachev, K. A. (2020). Effect of blasting on methane drainage in coal seam. *J. Min. Sci.* 56 (5), 793–796. doi:10.1134/S1062739120057129

Li, J., Tian, Y., Deng, Y., Zhang, Y., and Xie, K. (2020). Improving the estimation of greenhouse gas emissions from the Chinese coal-to-electricity chain by a bottom-up approach. *Resour. Conservation Recycl.* 167, 105237. doi:10.1016/j.resconrec.2020.105237

Li, T., Wu, B., and Lei, B. (2019). Study on the optimization of a gas drainage borehole drainage horizon based on the evolution characteristics of mining fracture. *Energies* 12, 4499. doi:10.3390/en12234499

Li, X., Zhang, J., Li, R., Qi, Q., Zheng, Y., Li, C., et al. (2021). Numerical simulation research on improvement effect of ultrasonic waves on seepage characteristics of coalbed methane reservoir. *Energies* 14, 4605. doi:10.3390/en14154605

Liang, W., Yan, J., Zhang, B., and Hou, D. (2021). Review on coal bed methane recovery theory and technology: Recent progress and perspectives. *Energy & Fuels* 35 (6), 4633–4643. doi:10.1021/acs.energyfuels.0c04026

Liu, H. Y., Zhang, B. Y., Li, X. L., Liu, C. W., Wang, C., Wang, F., et al. (2022). Research on roof damage mechanism and control technology of gob-side entry retaining under close distance gob. *Eng. Fail. Anal.* 138, 106331. doi:10.1016/j.engfailanal.2022.106331

Liu, X., Jing, T., Lin, H., Xuan, D., Li, Y., and Xu, S. (2022). Morphological characteristics and permeability evolution of deep mine gas drainage boreholes. *Front. Earth Sci.* 10, 906923. doi:10.3389/feart.2022.906923

Lu, Z., Wang, L., Lv, M., Lei, Y., Wang, H., and Liu, Q. (2022). Experimental study on coal and gas outburst risk in strong outburst coal under different moisture content. *Front. Earth Sci.* 10, 782372. doi:10.3389/feart.2022.782372

Qi, Q., Guan, W., Li, X., Ge, Y., Nan, S., and Liu, H. (2021). Mechanism of increasing the permeability of water-bearing coal rock by microwave steam explosion. *Geofluids* 2021 (7), 1–13. doi:10.1155/2021/6661867

Shang, Z., Wang, H., Li, B., Cheng, Y., Zhang, X., et al. (2022). The effect of leakage characteristics of liquid CO2 phase transition on fracturing coal seam: Applications for enhancing coalbed methane recovery. *Fuel* 308, 122044. doi:10.1016/j.fuel.2021.122044

Sun, J., Li, G., and Wang, Z. (2018). Optimizing China's energy consumption structure under energy and carbon constraints. *Struct. Change Econ. Dyn.* 47, 57–72. doi:10.1016/j.strueco.2018.07.007

Wang, K., Tang, S., Zhang, S., Guo, Y., Lin, D., and Niu, Z. (2022). Numerical simulation of fracture propagation characteristics of hydraulic fracturing in multiple coal seams, eastern yunnan, China. *Front. Earth Sci.* 10, 854638. doi:10.3389/feart.2022.854638

Wang, L., Lu, Z., Chen, D., Liu, Q. q., Chu, P., Shu, L. y., et al. (2022). Safe strategy for coal and gas outburst prevention in deep-and-thick coal seams using a soft rock protective layer mining. *Saf. Sci.* 129, 104800. doi:10.1016/j.ssci.2020.104800

Yang, R., Ding, C., Yang, L., Lei, Z., Zhang, Z., and Wang, Y. (2018). Visualizing the blast-induced stress wave and blasting gas action effects using digital image correlation. *Int. J. Rock Mech. Min. Sci.* 112, 47–54. doi:10.1016/j.ijrmms.2018.10.007

Zhao, F., Sang, S., Han, S., Wu, Z., Zhang, J., Xiang, W., et al. (2022). Characteristics and origins of the difference between the middle and high rank coal in Guizhou and their implication for the cbm exploration and development strategy: A case study from dahebian and dafang block. *Energies* 15, 3181. doi:10.3390/en15093181

Zuo, S., Zhang, L., and Deng, K. (2022). Experimental study on gas adsorption and drainage of gas-bearing coal subjected to tree-type hydraulic fracturing. *Energy Rep.* 8, 649–660. doi:10.1016/j.egyr.2021.12.003